



Article

Citrus aurantium 'Crispifolia' Essential Oil: A Promise for Nutraceutical Applications

Michela Di Napoli ^{1,†}, Giusy Castagliuolo ^{1,†}, Natale Badalamenti ², Viviana Maresca ¹, Adriana Basile ¹,
Maurizio Bruno ², Mario Varcamonti ¹ and Anna Zanfardino ^{1,*}

¹ Department of Biology, University of Naples Federico II, 80126 Naples, Italy

² Department of Biological, Chemical and Pharmaceutical Sciences and Technologies (STEBICEF), Università degli Studi di Palermo, Viale delle Scienze, Ed. 17, 90128 Palermo, Italy

* Correspondence: anna.zanfardino@unina.it

† These authors contributed equally to this work.

Abstract: Food waste is one of the main topics of various scientific studies of the last decade. In this regard, this work analyzed an essential oil (EO) extracted from the flavedo of *Citrus aurantium* 'Crispifolia' fruit. The analysis, performed by GC-MS, showed a chemically variegated chromatogram characterized by the presence of limonene (33.35%), but also by oxygenated monoterpenes such as β -linalool (7.69%), α -terpineol (7.06%), and geranyl acetate (10.12%). EO from the external part of the *C. aurantium* peel had several properties, including excellent antimicrobial and good antibiofilm activities. It also showed antioxidant activity in vitro and decreased the amount of cellular ROS, thus stimulating the catalytic activity of crucial enzymes involved in mitigating oxidative stress.

Keywords: *Citrus aurantium* 'Crispifolia'; essential oil; antimicrobial activity; antibiofilm effect; antioxidant properties



Citation: Di Napoli, M.; Castagliuolo, G.; Badalamenti, N.; Maresca, V.; Basile, A.; Bruno, M.; Varcamonti, M.; Zanfardino, A. *Citrus aurantium* 'Crispifolia' Essential Oil: A Promise for Nutraceutical Applications. *Nutraceuticals* **2023**, *3*, 153–164. <https://doi.org/10.3390/nutraceuticals3010011>

Academic Editor: Miquel Mulero

Received: 29 December 2022

Revised: 27 January 2023

Accepted: 8 February 2023

Published: 15 February 2023



Copyright: © 2023 by the authors. Licensee MDPI, Basel, Switzerland. This article is an open access article distributed under the terms and conditions of the Creative Commons Attribution (CC BY) license (<https://creativecommons.org/licenses/by/4.0/>).

1. Introduction

Citrus aurantium L., belonging to the family Rutaceae, is a species originating from the Asian continent [1,2] but today is distributed in all continents except Antarctica. Known as the bitter orange, it is a hybrid of *C. reticulata* Blanco and the pummelo *C. maxima* Burm. F. Merr. [1,3]. Even today, *C. aurantium* is used as a rootstock for obtaining different citrus fruits. Different studies have investigated the origin of this species. Scora [4] and Barrett & Rhodes [5] proposed the origin of this species from *C. reticulata* and *C. grandis*, results that were later supported by enzymatic studies [6] and RAPD and SCAR markers [7]. Different studies [7,8] demonstrated that the pummelo was the female parent of the bitter orange, excluding a hybrid originating from the sweet orange and the mandarin [9]. This result strongly argued that the pummelo was probably the maternal parent of the sour orange. The results obtained by Li et al. [10] strongly suggested that the mandarin was instead the "father" of the bitter orange, identifying more clearly the maternal and paternal origins of the bitter orange compared to all other previously collected scientific data.

In Italy and also in the Iberian Peninsula, the bitter orange is cultivated intensely, contributing 80% of the total production in Europe [11]. In addition to the production of juices and other food products (candies, granitas, etc.) from the bitter orange, its waste, mainly the peel and in particular the flavedo, can be used for the production of cosmetic and pharmaceutical products [12,13].

The flavedo of fruits of the genus *Citrus* are used to produce essential oils (EOs) that are chemically rich in limonene but have varying concentrations of other terpenoids, such as linalool, β -myrcene, and α -terpineol. However, the composition is dependent on various factors, such as harvest year [14], harvest date [15], cultivar [16], and extraction system [17]. In this context, the chemical composition of an EO from the Sicilian cultivar *C. aurantium* 'Crispifolia' Risso & Poit. was investigated by GC-MS. This cultivar is known by the local

name “*Aranciu amaru a fogghi rizzi*” because it has curled, dense leaves, and small fruit that are oval-oblong in shape. The EO of this fruit species is known for its antimicrobial properties [18]. *C. aurantium* EO showed good biofilm activity, and it is known that several plant species produce EOs capable of inhibiting biofilm formation [19]. Another important aspect concerns the antioxidant capacity of *C. aurantium* essential oil, which reduced the concentration of H₂O₂ and ABTS in vitro. In polymorphonuclear blood cells, it inhibited the production of oxygen free radicals and enhanced the catalytic effect of enzymes such as catalase and superoxide dismutase, which is of fundamental importance in processes that induce oxidative stress.

2. Materials and Methods

2.1. Plant Material and Isolation of Essential Oil

The fruit of *C. aurantium* ‘Crispifolia’ Risso & Poit. cultivar, collected in the Botanical Garden of Palermo (38°06′48.39″ N; 13°22′21.68″ E), Italy, was harvested in the first days of January 2020. A sample was accurately identified by Prof. Rosario Schicchi and deposited in the Mediterranean Herbarium of the same Botanical Garden with Voucher No. 109738.

The EO was extracted using a Clevenger apparatus with the procedure reported by European Pharmacopoeia 10.3.2020 [20]. The flavedo was acquired from twenty *C. aurantium* ‘Crispifolia’ fruit (111 g) collected from the only tree specimen present in the Botanical Garden of Palermo by manually peeling the fruit, which was then ground and subjected to hydrodistillation for 3 h. The obtained yield was 2.28% (*v/w*).

2.2. GC-MS Analysis

The experimental procedure was carried out as described by Badalamenti et al. [21] for the chemo-qualitative determination of *C. aurantium* ‘Crispifolia’ EO. A 1 µL diluted sample of EO (1/100 *v/v*, in *n*-pentane) was injected at 250 °C in splitless mode. GC-MS analysis was performed on an Agilent 6850 Ser. II apparatus fitted with a fused silica DB-5MS apolar capillary column (30 m × 0.25 mm, 0.33 µm film thickness) and coupled to an Agilent Mass Selective Detector MSD 5973 with an ionization voltage of 70 eV, electron multiplier energy of 2000 V, and transfer line temperature of 295 °C. Helium was used as the carrier gas (1 mL/min). Identification of compounds was carried out using NIST 11, Wiley 9, FFNSC 2, and Adams databases. The identifications were confirmed by linear retention indices with those available in the literature by the SciFinder database. The retention indices were determined in relation to a homologous series of *n*-alkanes (C₈–C₄₀) injected under the same operating conditions. Relative component concentrations were calculated based on GC peak areas without using correction factors.

2.3. Bacterial Strains

Gram-negative strains (*Escherichia coli* DH5α, *Pseudomonas aeruginosa* PAOI ATCC 15692, and *Salmonella* Typhimurium ATCC14028) and Gram-positive strains (*Staphylococcus aureus* ATCC6538P, *Bacillus cereus* ATCC10987, and *Mycobacterium Smegmatis* mc²155) were used to evaluate antimicrobial activity. *Mycobacterium Smegmatis* mc²155 was used to evaluate antibiofilm activity.

2.4. Antibacterial Tests

The antibacterial activity of the essential oil of *C. aurantium* was evaluated utilizing the inhibition halo experiment method with modifications [22]. EO activity was assessed in different quantities: 1, 10, and 50 µL of 22 mg/mL stock solution. The negative control was 50 µL dimethyl sulfoxide (DMSO) diluted in distilled water (40% *v/v*), which was also used to resuspend the *C. aurantium* EO. The antibiotic ampicillin (1 µL of 22 mg/mL stock solution) was used as the positive control. After incubation overnight at

37 °C, the halos were measured and antimicrobial activity was calculated according to the following formula [23]:

$$AU/mL = \frac{\text{Diameter of the zone of clearance (mm)} \times 1000}{\text{Volume taken in the well } (\mu\text{L})}$$

The cell viability of the indicator strains was used to quantitatively test the antibacterial properties of the EO. Different amounts of EO (1, 10, 100, and 200 µg/mL) were given to the indicator strains, using the same negative control as in the inhibition halo experiments. We used several antibiotics as positive controls, based on the resistance of the bacterial strains. In particular, we used 8, 24, 120, and 250 µg/mL ampicillin against *S. aureus*, *B. cereus*, *E. coli*, and *S. Typhimurium*, respectively. For *P. aeruginosa*, we used colistin at 2 µg/mL, while for *M. smegmatis*, we used rifampicin at 20 µg/mL.

The number of colonies present in the experimental control (samples consisting of cells plus PBS) were compared to the those in the treated samples [24]. Each test was performed at least three times (*p* value < 0.05).

2.5. MIC Experiment

Minimal inhibitory concentrations of *C. aurantium* EO against all indicator strains were determined according to the microdilution method established by the Clinical and Laboratory Standards Institute (CLSI). An aliquot of $\sim 5 \times 10^5$ CFU/mL of each indicator strain was added to 95 µL of Mueller-Hinton broth (CAM-HB; Difco) supplemented or not with various concentrations (1–200 µg/mL) of *C. aurantium* EO [25]. Each test was performed at least three times.

2.6. Antibiofilm Inhibition Test

A colorimetric assay was performed in order to assess *M. Smegmatis* biofilm inhibition. Microstyrene wells were filled to 1 mL in volume. Bacterial cells and medium plus DMSO was used as the negative control, cells treated with the antibiotic kanamycin (2 µg/mL) was used as the positive control, and the treated samples contained prokaryotic cells and EO (1, 2.5, 5, and 10 µg/mL). The plate was incubated at 37 °C for 36 h [26]. The percentage of biofilm formation was calculated by dividing the optical density values of the samples treated with EO and untreated samples.

2.7. Fluorescence Microscopy Experiment

Aliquots (100 µL) of *E. coli* DH5α and *S. aureus* ATCC6538P cells were placed in the dark for 2 h at 37 °C with stirring in the presence or absence of *C. aurantium* EO, at a concentration of 200 µg/mL. Samples were observed using an Olympus BX51 fluorescence microscope (Olympus, Tokyo, Japan) using a DAPI filter (excitation/emission: 358/461 nm) [27].

2.8. ABTS Scavenging Properties

The ABTS radical scavenging test was conducted according to the protocol cited by Napolitano et al. [28] with some modifications. A 1 mL aliquot of ABTS solution was added to 100 µL of EO (1, 10, 100, 200, 400, 500, and 1000 µg/mL). Each test was performed at least three times.

2.9. Hydrogen Peroxide Scavenging Test

The determination of the H₂O₂ scavenging capacity was measured by the decrease in the absorbance at 240 nm, as previously described in the literature [29]. Various concentrations of EO (1 to 1000 µg/mL) were incubated in 1 mL of hydrogen peroxide solution at room temperature. After half an hour, the hydrogen peroxide concentration was determined by measuring the absorbance. Each test was performed at least three times.

2.10. Cytotoxicity Tests

HaCat (human keratinocytes) and Caco-2 (intestinal epithelial cells) cell lines were used for the cytotoxicity tests. Cells were cultured at 37 °C in a humidified atmosphere under 5% CO₂ for 24 and 48 h. EO (10 to 1000 µg/mL) was added in complete growth medium (DMEM) for the cytotoxicity assay [30,31]. Each experiment was performed in triplicate and the reported result was an average of three independent experiments.

2.11. ROS Generation and Antioxidant Enzyme Activity against Polymorphonuclear Leukocytes (PMN)

Healthy volunteers (females and males) who provided consent underwent whole blood sampling in the morning.

PMNs were isolated following the protocol described by Badalamenti et al. [24]. PMNs were treated with *C. aurantium* EO at different concentrations (1, 10, 100, and 200 µg/mL) without or with opsonized zymosan (OZ; 0.5 mg/mL) for 6 h and then incubated with 2',7'-dichlorodihydrofluoresceine diacetate (DCFH-DA; final concentration 10 µM) for 15 min at 37 °C [32]. Commercial kits (BioAssay System, San Diego, CA, USA) were used to determine superoxide dismutase (SOD) and catalase (CAT) activities in PMN cells [33].

2.12. Statistical Analysis

The data shown in Figures 5 and 7 (values are presented as mean and standard error; numbers not accompanied by the same letter are significantly different at a *p* value < 0.05) were examined by one-way analysis of variance (ANOVA), followed by Tukey's multiple comparison post-hoc test.

3. Results and Discussion

3.1. Composition of the Essential Oil

Hydrodistillation of the flavedo of *C. aurantium* 'Crispifolia' fruit produced an EO with a strong yellow-orange hue and strong sour aroma. The chemical composition of this EO was previously described and reported by Badalamenti et al. [34]. As can be seen in the Table 1, the EO was characterized by a predominant component, limonene (33.35%), which contributed to almost all hydrocarbon monoterpenes (36.21%), but the main chemical class was oxygenated monoterpenes (44.79%). Regarding the latter, bergamol (6.77%), neryl acetate (6.28%), geranyl acetate (10.12%), α -terpineol (7.06%), and β -linalool (7.69%) were the main components. Both oxygenated and hydrocarbon sesquiterpenes and other compounds were present in minimal quantities (3.03–4.57%). The entire chemical composition of the EO is reported in Table 1. Based on these observations, the antimicrobial, antibiofilm, and antioxidant potential of *C. aurantium* 'Crispifolia' EO was explored.

Table 1. Chemical composition of the EO of the flavedo of *C. aurantium* 'Crispifolia' from Palermo, Sicily (Italy).

No.	Compounds	LRI _{exp} ^A	LRI _{lit} ^B	A ^C (%)
1	β -Pinene	977	981	0.91 ^d
2	β -Myrcene	990	994	1.95 ^f
3	Limonene	1031	1028	33.35 ^f
4	<i>n</i> -Octanol	1070	1078	1.59 ^a
5	β -Linalool	1098	1101	7.69 ^a
6	α -Terpineol	1189	1194	7.06 ^a
7	<i>cis</i> -Geraniol	1229	1235	1.63 ^a
8	β -Citral	1238	1242	1.88 ^a
9	Bergamol	1256	1258	6.77 ^a
10	<i>trans</i> -Geraniol	1259	1267	3.36 ^a
11	Neryl acetate	1365	1366	6.28 ^a
12	Geranyl acetate	1386	1392	10.12 ^a
13	<i>n</i> -Decyl acetate	1402	1406	1.44 ^a
14	Caryophyllene	1419	1423	1.00 ^a
15	Germacrene D	1480	1485	3.48 ^a
16	<i>trans</i> -Nerolidol	1550	1554	4.57 ^a

Table 1. *Cont.*

No.	Compounds	LRI _{exp} ^A	LRI _{lit} ^B	A ^C (%)
	Monoterpene Hydrocarbons			36.21
	Oxygenated Monoterpenes			44.79
	Sesquiterpene Hydrocarbons			4.48
	Oxygenated Sesquiterpenes			4.57
	Others			3.03
	Total			93.08

^A Linear retention index, obtained through the modulated chromatogram, reported for DB-5MS apolar column;

^B Linear retention index reported for DB-5MS column or equivalents reported in the literature; ^C Content is the peak volume percentage of compounds in the essential oil sample; Results followed by different letters in a same line are significantly different ($p < 0.05$) by Tukey's multiple range test.

3.2. Antimicrobial Activity Tests

To confirm the literature hypotheses [35] in which EOs extracted from similar plants possessed antimicrobial activity, inhibition halo experiments were performed according to the modified Kirby and Bauer protocol [22]. Figure 1 shows the relationship between the widths of the bacterial growth inhibition halos of two model indicator strains (*E. coli* and *S. aureus*) and the amount of EO spotted on a plate containing rich agar medium. As can be seen in the bar graph, the antimicrobial activity was directed against both bacterial strains and showed a proportionality between the size of the halo and quantity of EO (Samples 1, 2, and 3). The antibiotic ampicillin was used as a positive control and DMSO, which did not inhibit microbial growth, was used as a negative control.

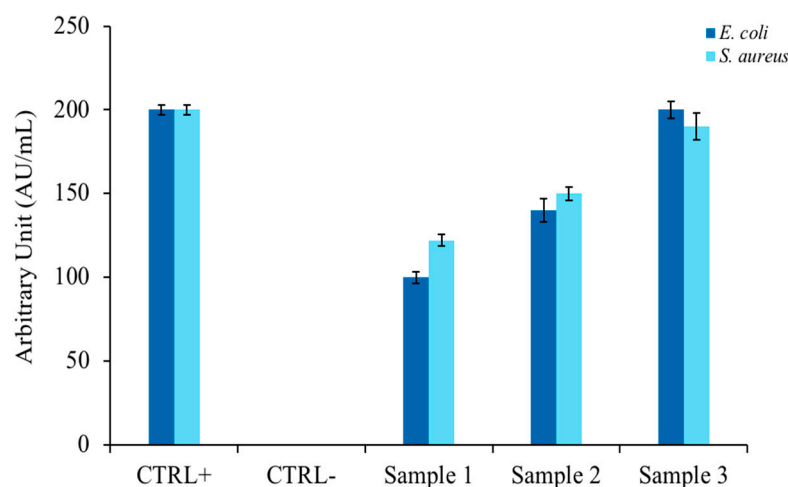


Figure 1. Determination of bacterial growth inhibition halo, expressed in arbitrary units. The histogram represents the zone of inhibition, expressed in AU/mL, of *C. aurantium* 'Crispifolia' against *E. coli* and *S. aureus*. Samples 1, 2, and 3 represent 1, 10, and 50 μ L of *C. aurantium* 'Crispifolia' EO, respectively. Positive control is ampicillin, negative control is DMSO (40%). The values are expressed as means of three different experiments; standard deviations are always less than 10%.

It was decided to extend the panel of indicator strains to include three Gram-negative bacteria (*E. coli*, *P. aeruginosa*, and *S. Typhimurium*) and three Gram-positive bacteria (*S. aureus*, *B. cereus*, and *M. smegmatis*). In addition to *E. coli*, we used *P. aeruginosa*, a well-known opportunistic pathogen that is capable of infecting small skin wounds [36,37] and responsible for intestinal infections [38]. *S. Typhimurium* was chosen because this serotype is also at the origin of numerous episodes of foodborne illness that have occurred in recent years in various European and non-European countries. Additionally, epidemiological evidence has demonstrated its close correlation with the swine supply chain [39]. Among Gram-positive bacteria, in addition to the use of *M. smegmatis* as a model strain for the formation of bacterial biofilms, we used *S. aureus*, an opportunistic pathogen involved in foodborne illness that normally resides on the skin of mammals and is therefore capable

of infecting small lesions very quickly [37,38]. We also used *B. cereus*, which produces two types of toxins: the first is stable to heat and causes vomiting, while the second is labile to heat and responsible for a form of diarrhea in unsuitable environmental conditions [40]. As shown in Figure 2, the dose-response curves indicate a proportionality between the concentration of EO and bacterial survival. The maximum EO concentration (200 µg/mL) reduced almost all bacterial strains by more than 50%. The most sensitive strains were represented by *E. coli* and *S. aureus*.

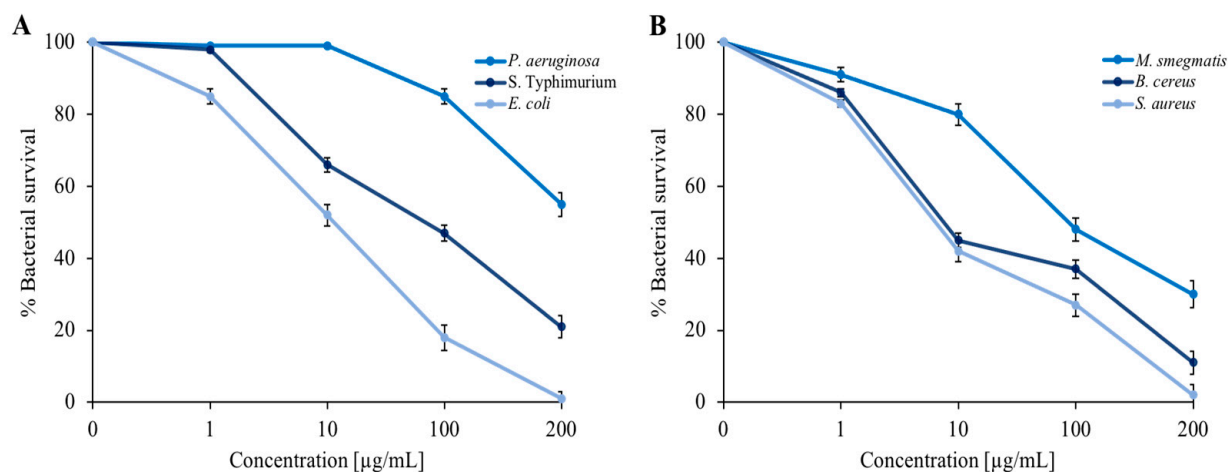


Figure 2. Determination of *C. aurantium* 'Crispifolia' EO antimicrobial activity against (A) *P. aeruginosa*, *S. Typhimurium*, and *E. coli*; and (B) *S. aureus*, *M. smegmatis*, and *B. cereus*. The assays were performed in three independent experiments. p value < 0.1.

Table 2 shows the MIC values obtained using the microdilution method. As expected from previous experiments, the lowest MIC values were determined against *E. coli* and *S. aureus*. This result, in accordance with the previous results, confirmed that the antimicrobial action of *C. aurantium* EO was directed against both Gram-positive and Gram-negative bacteria.

Table 2. Determination of minimum concentration values (MIC) inhibiting bacterial growth. The MIC₁₀₀ is expressed in µg/mL of *C. aurantium* 'Crispifolia' EO against the indicator strains. The values were obtained from a minimum of three independent experiments.

Strains	MIC ₁₀₀ [µg/mL]
<i>E. coli</i> DH5α	200
<i>P. aeruginosa</i> PAO1 ATCC 15692	>200
<i>S. Typhimurium</i> ATCC14028	>200
<i>S. aureus</i> ATCC6538P	200
<i>B. cereus</i> ATCC10987	>200
<i>M. smegmatis</i> MC ² 155	>200

In order to obtain some information about the mechanism of action of *C. aurantium* EO against the model strains, fluorescence microscopy was performed. Figure 3 shows optical (panels A, C, E, and G) and fluorescence microscope images (panels B, D, F, and H). EO at 200 µg/mL was administered to prokaryotic cells and two dyes were added. DAPI (4',6-diamidino-2-phenylindole) is a blue fluorescent stain that strongly binds to adenine-thymine-rich regions in the DNA. Because DAPI can pass through intact cell membranes, it is a marker of cell viability. PI (propidium iodide) cannot pass through intact cell membranes, so it is a marker of dead cells, showing a red color through damaged membranes.

E. coli bacterial cells treated with *C. aurantium* EO (panel C) appeared to be intact and dark gray, similar to the control cells under the same conditions (panel A). In panel D, the treated *E. coli* cells appeared blue, similar to the respective control cells (panel B). *S. aureus* cells treated with the maximum EO concentration (panel G) used for the other

experiments (200 µg/mL) had the same morphological features as the control cells (panel F). Furthermore, treated *S. aureus* cells (panel H) appeared blue, similar to the control cells (panel F). In conclusion, we hypothesize that the bacterial membrane was still intact after the administration of *C. aurantium* EO. Several studies reported that compounds present in the oil enter the bacterial cell, causing damage [41].

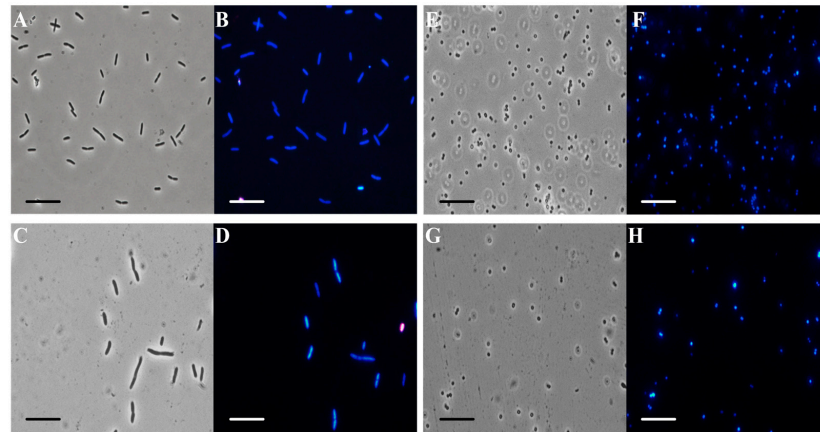


Figure 3. Analysis by fluorescence microscopy. Panels show *E. coli* bacterial cells (A–D) and *S. aureus* bacterial cells (E–H). Panels (A,C,E,G) show the cells observed under the optical microscope, and panels (B,D,F,H) show the cells observed under the fluorescence microscope. Untreated bacterial cells (A,B,E,F); cells treated with *C. aurantium* ‘Crispifolia’ EO (C,D,G,H). Scale bars: 1 µm (A–H).

3.3. Antibiofilm Tests

Some EOs can inhibit bacterial biofilm formation [26,42]. For this purpose, a colorimetric assay with crystal violet was performed. As shown in Figure 4, *C. aurantium* ‘Crispifolia’ EO had a good ability to inhibit *M. smegmatis* biofilm formation. The light blue curve shows a decrease in biofilm formation of more than 50% at the maximum EO concentration used. The positive control, represented by kanamycin (dark blue curve), and the negative control, represented by DMSO—in which the EO was dissolved (blue curve)—are also shown in the same figure. The EO was used in increasing concentrations, which did not cause mortality of the bacterial strain. The obtained effect was exclusively due to a decrease in the amount of biofilm, which was proportional to the increase in the EO concentration and not due to the death of the bacteria. Furthermore, *C. aurantium* ‘Crispifolia’ EO already showed antibiofilm activity at low concentrations. These aspects are very important for the potential use of *C. aurantium* EO, especially for use in cosmetics or as a food additive [43,44].

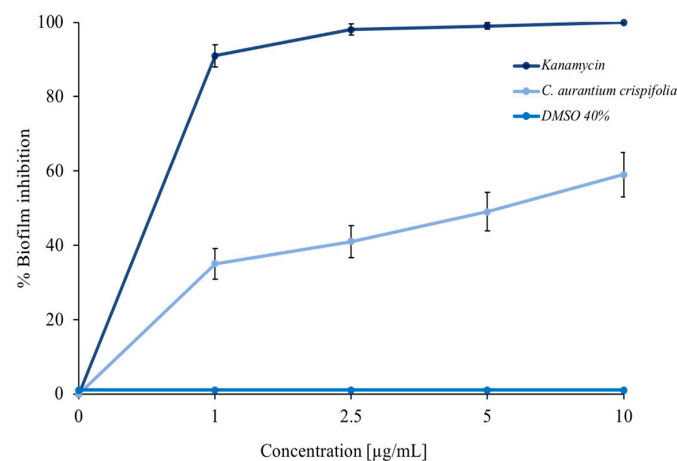


Figure 4. Percentage of *M. smegmatis* biofilm inhibition. Different concentrations of *C. aurantium* ‘Crispifolia’ EO were tested (x-axis). The assays were performed in three independent experiments. Standard deviations are always less than 5%.

3.4. Antioxidant Activity

The EO of *C. aurantium* ‘Crispifolia’ was rich in limonene (~33%), a hydrocarbon monoterpene that has an antioxidant activity [45]. Figure 5 shows the increasing ABTS and H₂O₂ radical scavenging activities as the EO concentration increased from 1 to 1000 µg/mL. The data shown in Figure 5 are expressed in Table 3 as IC₅₀ values, indicating the EO concentration that caused a 50% reduction in ABTS and H₂O₂ radicals. *C. aurantium* EO showed anti-H₂O₂ activity with an IC₅₀ value of 10 µg/mL and the lowest anti-radical effect (IC₅₀ value > 1000 µg/mL) for ABTS. Antioxidants are the chemical traps that inhibit oxidation, especially those used to counteract the deterioration of stored food products. Numerous antioxidants are commercially available for use in foods; however, natural antioxidants are preferred over synthetic ones because of their safety and functional and sensory properties. Monoterpenes are the major components of EOs of many plants known for their natural antioxidant potential [46]. The antioxidant activity possessed by our EO, along with the previous investigated activities, is of considerable importance for possible future nutraceutical applications.

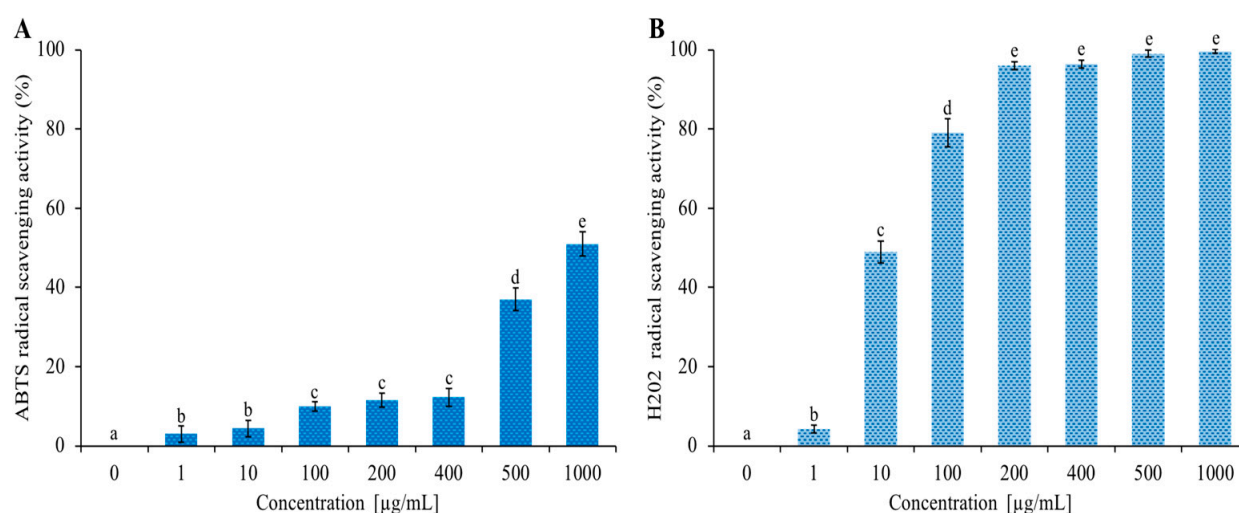


Figure 5. Determination of antioxidant activity of *C. aurantium* ‘Crispifolia’ EO. Panel (A) shows the abatement of ABTS radical activity reported as % of ABTS removed with respect to the control. Panel (B) shows the hydrogen peroxide scavenging activity reported as % of H₂O₂ removed relative to the control. Data were presented as mean and standard error and they were analyzed with a paired *t*-test. Bars not accompanied by the same letter were significantly different at *p* < 0.05.

Table 3. Concentration at 50% scavenging activity.

Sample	IC ₅₀ ABTS (µg/mL)	Sample	IC ₅₀ H ₂ O ₂ (µg/mL)
<i>C. aurantium</i> ‘Crispifolia’ EO	1000	<i>C. aurantium</i> ‘Crispifolia’ EO	10
Ascorbic acid	0.03	Resveratrol	0.05

3.5. Cytotoxic Activity

As shown in Figure 6, cytotoxicity tests were performed against HaCat cells (panel A) and Caco-2 cells (panel B) at different concentrations of *C. aurantium* EO (up to 1000 µg/mL). The MTT assay results after 24 and 48 h incubation with *C. aurantium* ‘Crispifolia’ EO revealed that the survival of treated cells was comparable to that of control cells. These tests led to the conclusion that this EO was non-toxic to the tested cell lines under these experimental conditions, which is very important for future applications in cosmetics and possibly as a food additive.

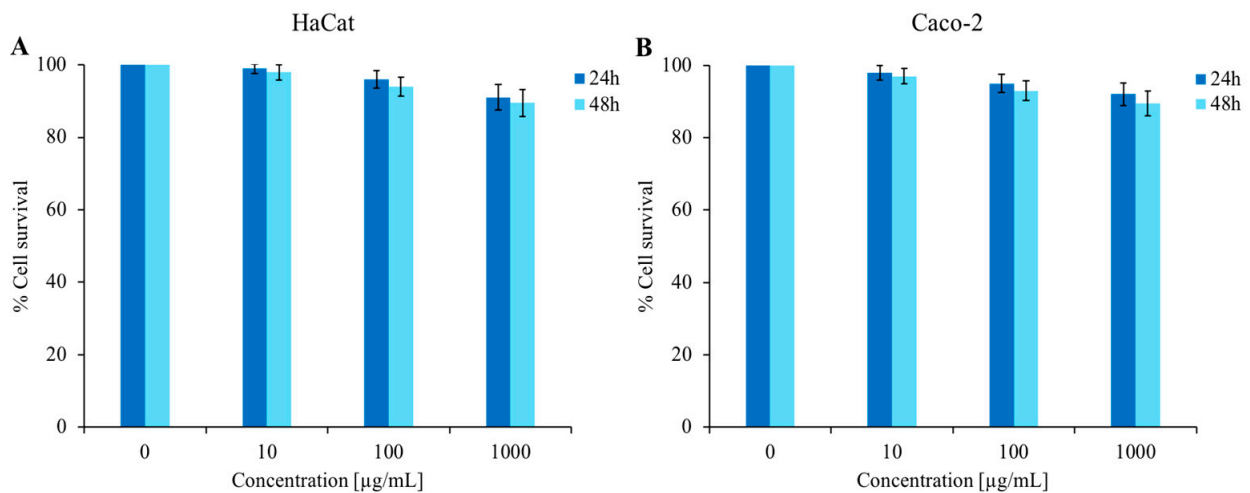


Figure 6. Determination of cytotoxic activity of *C. aurantium* ‘Crispifolia’ EO. Panel (A) shows the % cell survival of the HaCat cell line, while panel (B) shows the % cell survival of the Caco-2 cell line. Both cell lines were treated with different concentrations (*x*-axis) of EO for 24 and 48 h. % Cell survival is shown on the *y*-axis. The assays were performed in three independent experiments. Standard deviations are always less than 10%.

3.6. ROS Generation and SOD and CAT Activity in PMN

The variations in ROS levels and activities of antioxidant enzymes were evaluated in PMNs stressed with OZ (to induce oxidative stress) following treatment with *C. aurantium* ‘Crispifolia’ EO at different concentrations. As can be seen from Figure 7, there was an increase in ROS in PMNs stressed with OZ, but there was a gradual reduction in ROS following treatment with 100 and 200 µg/mL EO until reaching a situation comparable to the control (non-stressed PMNs). Regarding SOD and CAT, a gradual increase in enzyme activity was observed in PMNs treated with EO compared to untreated PMNs, probably to counteract the increase in ROS. The enzyme activity appeared to stabilize at 100 and 200 µg/mL *C. aurantium* EO.

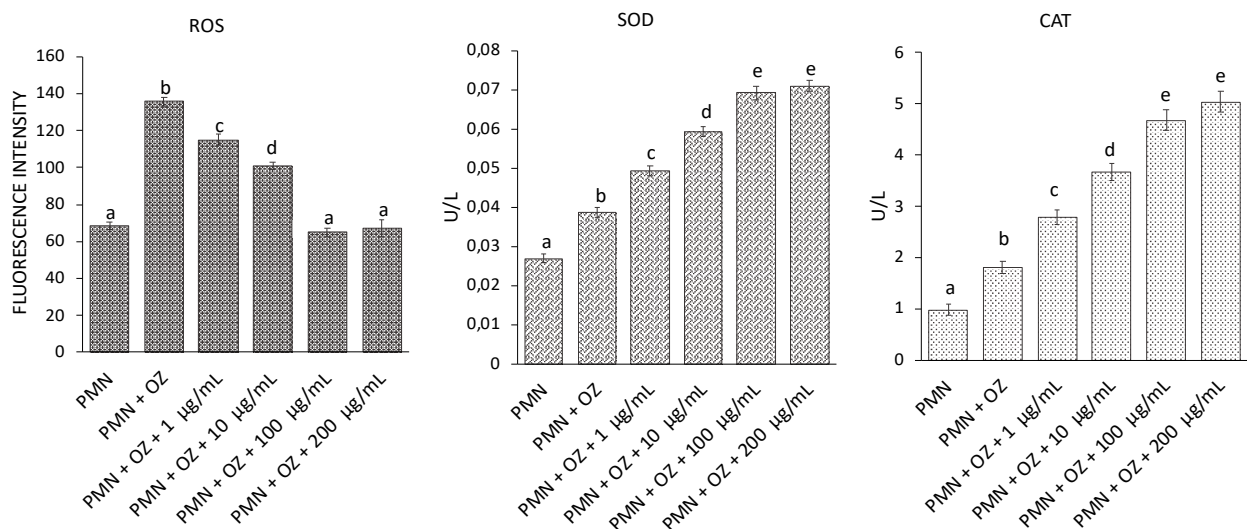


Figure 7. ROS generation and SOD and CAT activities in PMNs treated with EO of *C. aurantium* ‘Crispifolia’ at different concentrations (*x*-axis) with or without OZ. Data were presented as mean and standard error and they were analyzed with a paired t-test. Bars not accompanied by the same letter were significantly different at $p < 0.05$.

4. Conclusions

The EO of *C. aurantium* ‘Crispifolia’ was characterized by a high amount of the monoterpene hydrocarbon limonene (33.35%), but also by the presence of several oxygenated monoterpenes, such as bergamol (6.77%), neryl acetate (6.28%), geranyl acetate (10.12%), α -terpineol (7.06%), and β -linalool (7.69%).

The antimicrobial properties of this EO were investigated, demonstrating that this EO had effects against both Gram-negative and Gram-positive strains. It was also very effective against opportunistic pathogenic bacteria, which play a crucial role in food-borne or small skin wounds infections. We discovered considerable antibiofilm activity at low concentrations, indicating that the use of this EO in low concentrations could provide an important weapon against the formation of biofilms on skin wounds. The in vitro results with polymorphonuclear cells also enriched the findings of this study, demonstrating the antioxidant properties of this EO. Although it is quite complex to attribute a mixture of beneficial and protective biological activities for humans to a single compound, surely the combination of molecules present in *C. aurantium* EO makes it a natural source ideally suitable for nutraceutical application.

Author Contributions: Conceptualization: A.Z. and M.B.; methodology, V.M., M.D.N. and G.C.; formal analysis, M.D.N.; investigation, G.C., V.M. and M.D.N.; data curation, N.B.; writing—original draft preparation, M.V., A.B. and A.Z.; writing—review and editing, A.Z., M.V., V.M. and N.B.; supervision, A.Z. and M.B. All authors have read and agreed to the published version of the manuscript.

Funding: This research received external funding by National Biodiversity Future Center S.c.a.r.l., Piazza Marina 61 (c/o Palazzo Steri) Palermo, Italy, C.I. (No. CN00000033—CUP UNIPA B73C22000790001).

Institutional Review Board Statement: HaCat (human keratinocytes) cells were purchased from Cell Lines Service (CLS catalog number 300493); Caco-2 cells were purchased from ATCC (catalog number HTB-37).

Informed Consent Statement: Not applicable.

Conflicts of Interest: The authors declare no conflict of interest.

Sample Availability: A sample of this EO is available from the authors of the Department STEBICEF, University of Palermo, Palermo, Italy.

References

1. Swingle, W.T.; Reece, P.C.; Reuther, W.; Webber, H.J.; Batchelor, L.D. *The Citrus Industry*; University of California Press: Berkeley, CA, USA, 1967; pp. 190–430.
2. Ferrer, V.; Costantino, G.; Paoli, M.; Paymal, N.; Quinton, C.; Ollitrault, P.; Tomi, F.; Luro, F. Intercultivar diversity of sour orange (*Citrus aurantium* L.) based on genetic markers, phenotypic characteristics, aromatic compounds and sensorial analysis. *Agronomy* **2021**, *11*, 1084. [CrossRef]
3. Wu, G.A.; Prochnik, S.; Jenkins, J.; Salse, J.; Hellsten, U.; Murat, F.; Perrier, X.; Ruiz, M.; Scalabrin, S.; Terol, J.; et al. Sequencing of diverse mandarin, pummelo and orange genomes reveals complex history of admixture during *Citrus* domestication. *Nat. Biotechnol.* **2014**, *32*, 656–662. [CrossRef]
4. Scora, R.W. On the history and origin of *Citrus*. *Bull. Torrey Bot. Club* **1975**, *102*, 369–375. [CrossRef]
5. Barrett, H.C.; Rhodes, A.M. A numerical taxonomic study of affinity relationships in cultivated *Citrus* and its close relatives. *Syst. Bot.* **1976**, *1*, 105–136. [CrossRef]
6. Fang, D.Q. Intra- and intergeneric relationships of *Poncirus polyandar*: Investigation by leaf isozymes. *J. Wuhan Bot. Res.* **1993**, *11*, 34–40.
7. Nicolosi, E.; Deng, Z.N.; Gentile, A.; La Malfa, S.; Continella, G.; Tribulato, E. *Citrus* phylogeny and genetic origin of important species as investigated by molecular markers. *Theor. Appl. Genet.* **2000**, *100*, 1155–1166. [CrossRef]
8. Bayer, R.J.; Mabblerley, D.J.; Morton, C.; Miller, C.H.; Sharma, I.K.; Pfeil, B.E.; Rich, S.; Hitchcock, R.; Sykes, S. A molecular phylogeny of the orange subfamily (Rutaceae: Aurantioideae) using nine cpDNA sequences. *Amer. J. Bot.* **2009**, *96*, 668–685. [CrossRef]
9. Malik, M.N.; Scora, R.W.; Soost, R.K. Studies on the origin of the lemon. *Hilgardia* **1974**, *42*, 361–382. [CrossRef]
10. Li, X.; Xie, R.; Lu, Z.; Zhou, Z. The origin of cultivated *Citrus* as inferred from internal transcribed spacer and chloroplast DNA sequence and amplified fragment length polymorphism fingerprints. *J. Amer. Soc. Hort. Sci.* **2010**, *135*, 341–350. [CrossRef]
11. USDA Foreign Agricultural Service 2017. Available online: <https://www.fas.usda.gov> (accessed on 15 December 2022).

12. Bonesi, M.; Loizzo, M.R.; Leporini, M.; Tenuta, M.C.; Passalacqua, N.G.; Tundis, R. Comparative evaluation of petitgrain oils from six *Citrus* species alone and in combination as potential functional anti-radicals and antioxidant agents. *Plant Biosyst.* **2018**, *152*, 986–993. [[CrossRef](#)]
13. Russo, C.; Maugeri, A.; Lombardo, G.E.; Musumeci, L.; Barreca, D.; Rapisarda, A.; Cirimi, S.; Navarra, M. The second life of *Citrus* fruit waste: A valuable source of bioactive compounds. *Molecules* **2021**, *26*, 5991. [[CrossRef](#)] [[PubMed](#)]
14. Gioffrè, G.; Ursino, D.; Labate, M.L.C.; Giuffrè, A.M. The peel essential oil composition of bergamot fruit (*Citrus bergamia*, Risso) of Reggio Calabria (Italy): A review. *Emir. J. Food Agric.* **2020**, *32*, 835–845. [[CrossRef](#)]
15. Rowshan, V.; Najafian, S. Changes of peel essential oil composition of *Citrus aurantium* L. during fruit maturation in Iran. *J. Essent. Oil Bear.* **2015**, *18*, 1006–1012. [[CrossRef](#)]
16. Giuffrè, A.M.; Nobile, R. *Citrus bergamia*, Risso: The peel, the juice and the seed oil of the bergamot fruit of Reggio Calabria (South Italy). *Emir. J. Food Agric.* **2020**, *32*, 522–532. [[CrossRef](#)]
17. Ferhat, M.A.; Boukhatem, M.N.; Hazzit, M.; Meklati, B.Y.; Chemat, F. Cold pressing, hydrodistillation and microwave dry distillation of *Citrus* essential oil from Algeria: A comparative study. *Electron. J. Biol.* **2016**, *S1*, 30–41.
18. Teneva, D.; Denkova-Kostova, R.; Goranov, B.; Hristova-Ivanova, Y.; Slavchev, A.; Denkova, Z.; Kostov, G. Chemical composition, antioxidant activity and antimicrobial activity of essential oil from *Citrus aurantium* L Zest against some pathogenic microorganisms. *Z. Naturforsch. C* **2019**, *74*, 105–111. [[CrossRef](#)]
19. Lagha, R.; Ben Abdallah, F.; AL-Sarhan, B.; Al-Sodany, Y. Antibacterial and biofilm inhibitory activity of medicinal plant essential oils against *Escherichia coli* isolated from UTI patients. *Molecules* **2019**, *24*, 1161. [[CrossRef](#)]
20. European Pharmacopoeia 10.3. 2020. Determination of Essential Oils in Herbal Drugs, 2.8.12., 307. Available online: <https://www.edqm.eu/> (accessed on 10 December 2022).
21. Bancheva, S.; Badalamenti, N.; Bruno, M. The essential oil composition of the endemic plant species *Centaurea vandasii* and chemotaxonomy of section *Phalolepis* (Asteraceae). *Nat. Prod. Res.* **2021**. [[CrossRef](#)]
22. Bauer, A.W.; Kirby, W.M.; Sherris, J.C.; Turck, M. Antibiotic susceptibility testing by a standardized single disk method. *Am. J. Clin. Pathol.* **1966**, *45*, 493–496. [[CrossRef](#)]
23. Di Napoli, M.; Varcamonti, M.; Basile, A.; Bruno, M.; Maggi, F.; Zanfardino, A. Anti-*Pseudomonas aeruginosa* activity of hemlock (*Conium maculatum*, Apiaceae) essential oil. *Nat. Prod. Res.* **2019**, *33*, 3436–3440. [[CrossRef](#)]
24. Badalamenti, N.; Russi, S.; Bruno, M.; Maresca, V.; Vaglica, A.; Ilardi, V.; Zanfardino, A.; Di Napoli, M.; Varcamonti, M.; Cianciullo, P.; et al. Dihydrophenanthrenes from a Sicilian accession of *Himantoglossum robertianum* (Loisel.) P. delforge showed antioxidant, antimicrobial, and antiproliferative activities. *Plants* **2021**, *10*, 2776. [[CrossRef](#)] [[PubMed](#)]
25. Pota, G.; Zanfardino, A.; Di Napoli, M.; Cavasso, D.; Varcamonti, M.; D’Errico, G.; Pezzella, A.; Luciani, G.; Vitiello, G. Bioinspired antibacterial pva/melanin-TiO₂ hybrid nanoparticles: The role of poly-vinyl-alcohol on their self-assembly and biocide activity. *Colloids Surf. B Biointerfaces* **2021**, *202*, 111671. [[CrossRef](#)]
26. Di Napoli, M.; Maresca, V.; Varcamonti, M.; Bruno, M.; Badalamenti, N.; Basile, A.; Zanfardino, A. (+)-(E)-Chrysanthenyl acetate: A molecule with interesting biological properties contained in the *Anthemis secundiramea* (Asteraceae) Flowers. *Appl. Sci.* **2020**, *10*, 6808. [[CrossRef](#)]
27. Di Napoli, M.; Maresca, V.; Sorbo, S.; Varcamonti, M.; Basile, A.; Zanfardino, A. Proteins of the fruit pulp of *Acca sellowiana* have antimicrobial activity directed against the bacterial membranes. *Nat. Prod. Res.* **2021**, *35*, 2942–2946. [[CrossRef](#)]
28. Napolitano, A.; Di Napoli, M.; Castagliuolo, G.; Badalamenti, N.; Cicio, A.; Bruno, M.; Piacente, S.; Maresca, V.; Cianciullo, P.; Capasso, L.; et al. The chemical composition of the aerial parts of *Stachys spreitzenhoferi* (Lamiaceae) growing in Kythira Island (Greece), and their antioxidant, antimicrobial, and antiproliferative properties. *Phytochemistry* **2022**, *203*, 113373. [[CrossRef](#)]
29. Beers, R.; Sizer, I. A spectrophotometric method for measuring the breakdown of hydrogen peroxide by catalase. *J. Biol. Chem.* **1952**, *195*, 133–140. [[CrossRef](#)]
30. Vitiello, G.; Zanfardino, A.; Tammara, O.; Di Napoli, M.; Caso, M.F.; Pezzella, A.; Varcamonti, M.; Silvestri, B.; D’Errico, G.; Costantini, A.; et al. Bioinspired hybrid eumelanin-TiO₂ antimicrobial nanostructures: The key role of organo-inorganic frameworks in tuning eumelanin’s biocide action mechanism through membrane interaction. *RSC Adv.* **2018**, *8*, 28275–28283. [[CrossRef](#)]
31. Zanfardino, A.; Bosso, A.; Gallo, G.; Pistorio, V.; Di Napoli, M.; Gaglione, R.; Dell’Olmo, E.; Varcamonti, M.; Notomista, E.; Arciello, A.; et al. Human apolipoprotein E as a reservoir of cryptic bioactive peptides: The case of ApoE 133–167. *J. Pept. Sci.* **2018**, *24*, e3095. [[CrossRef](#)]
32. Manna, A.; Saha, P.; Sarkar, A.; Mukhopadhyay, D.; Bauri, A.K.; Kumar, D.; Das, P.; Chattopadhyay, S.; Chatterjee, M. Malabaricone-A induces a redox imbalance that mediates apoptosis in U937 Cell Line. *PLoS ONE* **2012**, *7*, e36938. [[CrossRef](#)]
33. Barbosa, P.O.; Pala, D.; Silva, C.T.; de Souza, M.O.; do Amaral, J.F.; Vieira, R.A.L.; de Freitas Folly, G.A.; Volp, A.C.P.; de Freitas, R.N. Açai (*Euterpe oleracea* Mart.) pulp dietary intake improves cellular antioxidant enzymes and biomarkers of serum in healthy women. *Nutrition* **2016**, *32*, 674–680. [[CrossRef](#)]
34. Badalamenti, N.; Bruno, M.; Schicchi, R.; Geraci, A.; Leporini, M.; Gervasi, L.; Tundis, R.; Loizzo, M.R. Chemical compositions and antioxidant activities of essential oils, and their combinations, obtained from flavedo by-product of seven cultivars of Sicilian *Citrus aurantium* L. *Molecules* **2022**, *27*, 1580. [[CrossRef](#)] [[PubMed](#)]
35. Hsouna, A.B.; Hamdi, N.; Halima, N.B.; Abdelkafi, S. Characterization of essential oil from *Citrus aurantium* L. flowers: Antimicrobial and antioxidant activities. *J. Oleo Sci.* **2013**, *62*, 763–772. [[CrossRef](#)]

36. Spernovasilis, N.; Psychogiou, M.; Poulakou, G. Skin manifestations of *Pseudomonas aeruginosa* infections. *Curr. Opin. Infect. Dis.* **2021**, *34*, 72–79. [[CrossRef](#)]
37. Serra, R.; Grande, R.; Butrico, L.; Rossi, A.; Settimio, U.F.; Caroleo, B.; Amato, B.; Gallelli, L.; de Franciscis, S. Chronic wound infections: The role of *Pseudomonas aeruginosa* and *Staphylococcus aureus*. *Expert Rev. Anti Infect. Ther.* **2015**, *13*, 605–613. [[CrossRef](#)]
38. Affhan, S.; Dachang, W.; Xin, Y.; Shang, D. Lactic acid bacteria protect human intestinal epithelial cells from *Staphylococcus aureus* and *Pseudomonas aeruginosa* infections. *Genet. Mol. Res.* **2015**, *14*, 17044–17058. [[CrossRef](#)]
39. Andreoli, G.; Merla, C.; Valle, C.D.; Corpus, F.; Morganti, M.; D'inciau, M.; Colmegna, S.; Marone, P.; Fabbi, M.; Barco, L.; et al. foodborne salmonellosis in italy: Characterization of *Salmonella enterica* Serovar Typhimurium and monophasic variant 4,[5],12:I–isolated from salami and human patients. *J. Food Protect.* **2017**, *80*, 632–639. [[CrossRef](#)]
40. Schoeni, J.L.; Lee Wong, A.C. Bacillus cereus food poisoning and its toxins. *J. Food Protect.* **2005**, *68*, 636–648. [[CrossRef](#)]
41. Nazzaro, F.; Fratianni, F.; De Martino, L.; Coppola, R.; De Feo, V. Effect of essential oils on pathogenic bacteria. *Pharmaceuticals* **2013**, *6*, 1451–1474. [[CrossRef](#)]
42. Di Napoli, M.; Castagliuolo, G.; Badalamenti, N.; Maresca, V.; Basile, A.; Bruno, M.; Varcamonti, M.; Zanfardino, A. Antimicrobial, antibiofilm, and antioxidant properties of essential oil of *Foeniculum vulgare* Mill. leaves. *Plants* **2022**, *11*, 3573. [[CrossRef](#)]
43. Borotová, P. Biological activity of *Citrus aurantium* var. *bergamia* essential oil as a food spoilage inhibitor. *Sci. Pap. Anim. Sci. Biotechnol.* **2021**, *54*, 117–120.
44. González-Mas, M.C.; Rambla, J.L.; López-Gresa, M.P.; Blázquez, M.A.; Granell, A. Volatile compounds in *Citrus* essential oils: A comprehensive review. *Front. Plant Sci.* **2019**, *10*, 12. [[CrossRef](#)]
45. Badalamenti, N.; Maresca, V.; Di Napoli, M.; Bruno, M.; Basile, A.; Zanfardino, A. Chemical composition and biological activities of *Prangos ferulacea* essential oils. *Molecules* **2022**, *27*, 7430. [[CrossRef](#)]
46. Graßmann, J. Terpenoids as plant antioxidants. *Vit Horm.* **2005**, *72*, 505–535.

Disclaimer/Publisher's Note: The statements, opinions and data contained in all publications are solely those of the individual author(s) and contributor(s) and not of MDPI and/or the editor(s). MDPI and/or the editor(s) disclaim responsibility for any injury to people or property resulting from any ideas, methods, instructions or products referred to in the content.